NASA DEVELOP National Program
Georgia – Athens

Fall 2022

Yellowstone Ecological Forecasting II

Assessing Change in Aspen Extent in Northern Yellowstone National Park

DEVELOP Technical Report

Final – November 17th, 2022

Vanessa Bailey (Project Lead)
Ryan Brinton
Samantha Snowden
Aliza White

Advisors:
Dr. Marguerite Madden, University of Georgia, Center for Geospatial Research (Science Advisor)
Joseph Spruce, Science Systems and Applications, Inc. (Science Advisor)

Previous Contributors:
Kyle Steen
Gabriella Boodhoo
Barry McLaughlin
Dr. Kunwar Singh, William & Mary, AidData, Global Research Institute (Science Advisor)

Fellow:
Sarah Payne (Georgia - Athens)

1. Abstract

Aspen stands in Yellowstone National Park have been indirectly affected by the removal and reintroduction of wolves in 1926 and 1995, respectively. The National Park Service has a strong interest in the trophic cascade of wolves, elk, and aspen due to their ecological importance. In partnership with Yellowstone National Park, Utah State University, and the University of Wisconsin–Stevens Point, this project analyzed data from 1954 and 2021 to determine change in aspen extent at a landscape scale. The team used historical aerial imagery to determine aspen stand extent in 1954 with particular focus on 113 belt transects provided by the team's partners. To determine aspen stand extent in 2021, the team processed Landsat 8 Operational Land Imager (OLI) and Sentinel-2 Multispectral Instrument (MSI) imagery using a random forest classification. The team then refined outputs with a phenological approach to distinguish between deciduous and evergreen vegetation. The team produced maps of aspen extent for 1954 and 2021. Despite limitations in scales of comparison, the results generally indicate a decline in aspen stand extent over time. This project provides greater context for monitoring aspen stands, understanding the landscape-scale impacts of wolf reintroduction, and communicating the trophic cascade story to the public.

Key Terms

Populus tremuloides, trophic cascade, random forest, phenology, aerial imagery, digitization, wolves

2. Introduction

2.1 Background Information

The impact of the removal and subsequent reintroduction of wolves (*Canis lupus*) on aspen (*Populus tremuloides*) in Yellowstone National Park has become a textbook example of a trophic cascade. Aspen plays an integral role within ecosystems by providing valuable habitat for wildlife, reducing the intensity of wildfires due to its relative fire resistance, promoting nutrient cycling, and supporting understory plant communities (Ripple & Beschta, 2012; Ripple & Larsen, 2001). Thus, the decline in aspen due to an increase in elk (*Cervus canadensis*) population caused by the extirpation of wolves in the park has had significant negative implications for biodiversity in the region (Brown et al., 2006). Since the reintroduction of the gray wolf in 1995, researchers theorized that predation and altered elk browsing behavior supported aspen regeneration in Yellowstone (Beschta & Ripple, 2016; Ripple & Larsen, 2000; Ripple et al., 2001). With increased predation on elk, a greater number of aspen saplings have been able to survive past the browsing height of ungulates (Painter et al., 2014). Understanding the unique dynamics between wolves, elk, and aspen in Yellowstone National Park could provide deeper insights to wildlife reintroductions and trophic dynamics.

Several past studies have employed remote sensing methods to assess aspen and trophic cascades. For example, a similar study in Montana used a regression tree classifier to successfully identify percentage of aspen extent (Hamilton et al., 2009). Other studies have used both historic and recent aerial photography to measure increases in aspen canopy coverage with decreased elk browsing (Larsen & Ripple, 2005). These previous studies illustrate initial success in using aerial photography and remote sensing techniques for aspen identification and monitoring. They also demonstrate benefits of integrating remote sensing into natural resource management decision-making.

The primary study area of the project was aspen stands associated with 113 20 x 1 m belt transects across a ~1000 km^2 range in northern Yellowstone National Park (Figure 1). These transects are also within the northern elk wintering range in Yellowstone. The landcover in the area is comprised of bare ground, grass, shrubs, conifers, aspen, and other deciduous species, like cottonwood and willow, which could have similar spectral signatures compared to aspen. Aspens are scattered across the landscape as individual stands or mixed with conifers and make up just 1% of landcover in Yellowstone National Park (Brown et al., 2006).

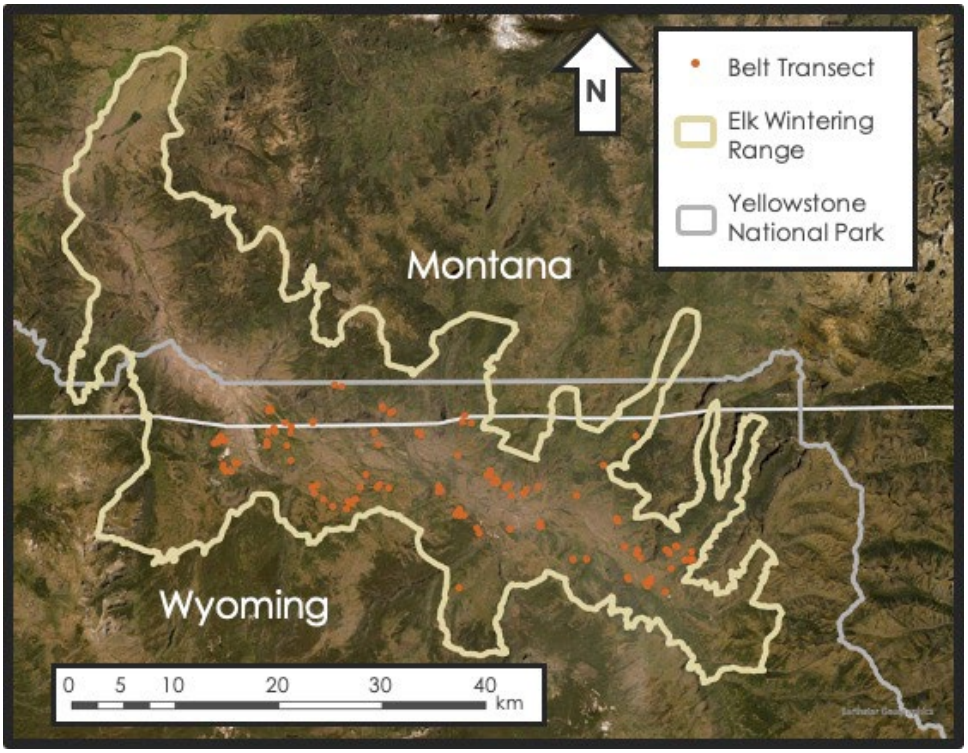

Figure 1. Location of belt transects and elk wintering range in northern Yellowstone National Park.

The Summer 2022 team conducted preliminary analysis of aspen and deciduous presence for several years from 1986 to 2019 across the elk wintering range (Steen et al., 2022). Differences in area of aspen coverage emerged due to the two approaches utilized: random forest and phenology. The random forest method used predictor variables and training points of a variety of landcover types to determine classification. The phenological approach used differences in normalized difference vegetation index (NDVI) between summer and fall to determine whether areas had deciduous or evergreen vegetation. NDVI for evergreen vegetation remains relatively stable over seasons while deciduous vegetation NDVI peaks in summer with greenness and drops in fall with leaf senescence. While the random forest method indicated a general decline in aspen extent, the phenological approach showed a relative increase with time (Steen et al., 2022). Several limitations, including the reliability of training points for years far before the satellite imagery used to identify landcover, influenced these results. Using both approaches in combination to increase confidence in classified areas, the trend showed a more subtle decline in aspen extent from 62.62 km^2 in 1986 to 21.12 km^2 in 2019 (Steen et al., 2022).

2.2 Project Partners & Objectives

The DEVELOP team partnered with collaborators based at Yellowstone National Park, Utah State University, and the University of Wisconsin–Stevens Point. The project's partners currently monitor 113 *in situ* belt transects with varying aspen presence. While the sample plots provide information on vegetative cover and aspen presence, they do not have sufficient detail across the northern Yellowstone region as a whole (Hamilton et al., 2009). Due to the limited span of the belt transects, the use of remote sensing technology could prove to be beneficial for studying the change in aspen extent across the landscape. The goal of the analysis was to quantify change in aspen extent in the context of elk and wolf dynamics in Yellowstone National Park. Park managers could then use the analysis to inform the conservation and management of aspen stands and wildlife. The partners were interested in building on the previous term's analysis of change in aspen extent across the northern Yellowstone range to include historical aerial imagery from 1954 and a refined analysis of 2021 aspen extent derived from satellite imagery. Consolidated maps provide partners with insight into aspen decline and regeneration in the context of elk and wolf dynamics,

which may inform restoration and management decision-making. Specifically, the partners aim to assess the connection between changes in aspen overstory and elk population dynamics in relation to wolf predation. Carnivore reintroduction is a controversial topic, and this project provides more context on the role of wolves in the Yellowstone ecosystem.

This project had several objectives that aimed to address the concerns of the partner organizations. The team georeferenced the earliest known historical aerial imagery of the study region and then digitized aspen extent for 1954, decades prior to wolf reintroduction. Using training points derived from high-resolution aerial imagery, the team refined the previous term's random forest and phenology approaches to model aspen extent in 2021. The team then produced maps and tables to visualize and quantify change in aspen extent over the study period.

3. Methodology

3.1 Data Acquisition

3.1.1 Historical Imagery

The team batch-downloaded scanned aerial imagery taken on September 24th, 1954, from the United States Geological Survey (USGS) EarthExplorer. The team selected 24 images that included at least one of the aspen belt transects provided by the partners. The scale of the selected imagery was 37400:1 and scanned at 1000 dots per inch, resulting in an approximate 1 m pixel size.

3.1.2 2021 Imagery

The team used Google Earth Engine (GEE) to obtain Landsat 8 Operational Land Imager (OLI) and Sentinel-2 Multispectral Instrument (MSI) surface reflectance imagery for 2021 between June and October. The spatial resolution of the Landsat 8 OLI imagery is 30 m, and Sentinel-2 MSI imagery is 10 m. The team selected cloudless, peak leaf change (fall) imagery for the random forest classification while cloudless, peak greenness (summer) and senescence (fall) imagery were used for the phenological method. Clouds were filtered in both image collections by removing images with significant cloud coverage in the elk wintering range. Since the team found cloudless imagery for the dates of interest, cloud masks were not necessary.

3.1.3 Planet Imagery

The team obtained 3 m spatial resolution images for both summer and fall 2021 from PlanetScope to process and send to partners for training point identification. Imagery was filtered to exclude images with greater than twenty percent cloud cover and to only include surface reflectance images. The team uploaded a shapefile of the elk wintering range provided by the partners and selected images that would encompass the entire area of interest. The team selected imagery from June 21 and October 3, 2021. These dates were selected because they had low cloud cover (zero percent) and full coverage of the study area after tiles from the same date were mosaicked together.

3.1.4 Ancillary Datasets

Partners from Utah State University provided the team with training points for several landcover classes across the elk wintering range. The partners identified landcover types including aspen, conifers, bare ground, and water using high-resolution PlanetScope imagery from 2021 and Sentinel-2 MSI imagery from September 27, 2021, that showed leaf color change, and first-hand knowledge of the landscape. The partners also provided the locations of the 113 belt transects where aspen have been monitored since 1999. In GEE, the team acquired a Digital Elevation Model (DEM) for the region from the USGS 3D Elevation Program (3DEP) with a 1/3 arc-second (~10m) resolution to use for predictors in the random forest model.

3.2 Data Processing

3.2.1 Historical Imagery

The team loaded USGS aerial images for 1954 into ArcGIS Pro 3.0.2 and individually georeferenced them to be properly adjusted to the study area. Georeferencing involves relating the internal coordinate system of a digital map or image to a geographic coordinate system by matching distinguishable points between the two.

The team georeferenced each image as a second order polynomial to static land features, such as ridges and rock formations, that have remained relatively stable since 1954, starting in the center and then moving to the edges of the image. To choose control points, the team compared the 1954 aerial imagery to National Agricultural Imagery Program (NAIP) imagery from 2019.

3.2.2 Planet Mosaicking

The team loaded PlanetScope imagery into GEE as several individual tiles of multiple image collections for June and a single image collection for October. To provide the partners with a single image for identifying training points, the team first merged the June imagery into a single image collection using the merge function sequentially until all image collections were combined. The team then mosaicked the final image collections into single images for both June and October. The June and October images were then clipped to the study area of the elk wintering range.

3.2.3 DEM Metrics

The team used the DEM that covered the greater study area to generate additional predictors. Slope and aspect layers were created using the associated Terrain functions in GEE. The team created these variables to increase the number of predictors fed into the random forest model and ideally improve results for landcover classification within the study area.

3.2.4 Google Earth Engine

Within GEE, Landsat 8 OLI and Sentinel-2 MSI imagery were filtered for specific dates, the area of interest (northern elk wintering range), and minimal cloud cover (less than 20 percent). For the random forest model, the team used a Landsat 8 OLI mosaicked image from September 25th to October 25th, 2021, and a Sentinel-2 MSI image from September 27, 2021, in which the peak fall color of deciduous vegetation was visible. For the summer phenology, the specific imagery used from Landsat 8 OLI and Sentinel-2 MSI ranged temporally from June 10th to July 20th, 2021. Imagery from September 25th to October 25th, 2021, was used for the fall phenology for both sensors. If suitable (i.e., cloudless) imagery was not available for the entire region for a specific date, imagery from multiple dates were mosaicked together.

3.2.5 Derived Indices

The team derived several indices from the Landsat 8 OLI and Sentinel-2 MSI 2021 imagery. Indices like NDVI, Enhanced Vegetation Index (EVI), and Tasseled Cap Transformations (TCTs), were used as predictors, along with the original bands, in the random forest classification. NDVI serves as a proxy for vegetation health and is calculated by taking the difference between near infrared light (NIR) and visible red light (Red) over their sum (Equation 1; Rouse et al., 1974). NDVI was needed for both methods for 2021, as a predictor in the random forest classification and as the metric used to quantify change between summer and fall in the phenological approach. NDVI is a robust vegetation index that captures changes in absorption and reflectance of red and NIR bands.

$$NDVI = \frac{(NIR - Red)}{(NIR + Red)} \quad (1)$$

EVI supplemented NDVI as another predictor in the random forest approach. EVI is a more sensitive vegetation index than NDVI that can better differentiate variations in dense canopies by correcting for atmospheric distortions and canopy background noise. Near-infrared, red, and blue bands and several coefficients influence EVI (Equation 2; Huete et al., 1994). G is a gain factor, C1 and C2 are atmospheric resistance coefficients, and L is a canopy background adjustment value. The coefficient values determined for this project were G = 2.5, C1 = 6, C2 = 7.5, and L = 1. These values were taken from the Moderate Resolution Imaging Spectroradiometer (MODIS) EVI algorithm and adopted for use in these satellite calculations.

$$EVI = G \cdot \left(\frac{(NIR - Red)}{(NIR + C1 \cdot Red - C2 \cdot Blue + 1)} \right) \quad (2)$$

The first three band components of TCTs were used as predictors in the random forest approach and provide information on brightness, greenness, and wetness (Equations 3-5; Kauth & Thomas, 1976). Brightness is a measure of bare ground, greenness a measure of green vegetation, and wetness a measure of moisture and water. TCT coefficients (C) are satellite sensor-specific (Baig et al. 2014; Lamqadem, Saber, & Pradhan, 2018) and produce weighted sums of the satellite bands. The satellite bands used are the 3 true color bands (red, blue, and green; RGB), near infrared band (NIR), and shortwave infrared bands (SWIR1 and SWIR2).

$$Brightness\,(b) = C_b1(B) + C_b2(G) + C_b3(R) + C_b4(NIR) + C_b5(SWIR1) + C_b6(SWIR2) \quad (3)$$

$$Greenness\,(g) = C_g1(B) + C_g2(G) + C_g3(R) + C_g4(NIR) + C_g5(SWIR1) + C_g6(SWIR2) \quad (4)$$

$$Wetness\,(w) = C_w1(B) + C_w2(G) + C_w3(R) + C_w4(NIR) + C_w5(SWIR1) + C_w6(SWIR2) \quad (5)$$

3.3 Data Analysis

3.3.1 Digitization

Following the guidance of the project's science advisors and partners in identifying historic aspen stands based on texture and shadows in the imagery, the team digitized aspen extent in the stands encompassing the provided 113 belt transects for 1954 in ArcGIS Pro 3.0.2, creating a shapefile containing the 113 digitized aspen stands. These were grouped based on confidence levels of the accuracy of the digitization, with greatest confidence defined as group 1, moderate confidence as group 2, and least confidence as group 3. The team then manually shifted the digitized stands individually to better line up with the modern-day Sentinel-2 imagery. The digitized stands did not align properly initially due to the inherent limitations of georeferencing.

3.3.2 Random Forest

A random forest model is a commonly used supervised machine-learning algorithm that builds decision trees to classify data into groups suggested by most trees (Hayes et al., 2014). The team used predictor variables of color bands, near infrared, shortwave infrared, elevation, slope, aspect, NDVI, EVI, and TCTs, as well as partner-provided training points to run the model. PlanetScope imagery was used solely to obtain accurate landcover training points, while the random forest analysis was run using both 30 m Landsat 8 OLI imagery and 10 m Sentinel-2 MSI imagery separately for comparison. 70% of the partner-provided points were used to train the random forest model and 30% were used to validate its classification accuracy. Training points were locations of various land cover classes (water, bare ground, aspen, conifers, grass, shrubs, and other deciduous tree species). Grasslands, shrublands, cottonwood, and willow were combined into one aggregate class both for consistency with the first term's methodology and because it increased model's accuracy. The team analyzed the role of different predictors through variable of importance graphs and assessed model accuracy with Cohen's kappa statistics and confusion matrices for 2021. The team exported a layer of modeled aspen extent and compared it with historic stands in ArcGIS Pro 3.0.2.

3.3.3 Phenology

The team integrated the same partner-provided data points to calculate accurate NDVI values for aspen and conifers for all of 2021. Aspen and conifers are distinguishable because aspens are deciduous and show a

pronounced change in NDVI between summer and fall while conifers are evergreen and have a relatively stable NDVI. The team plotted NDVI for the two landcover types to determine the time of peak greenness and senescence and establish a threshold value to distinguish deciduousness from other landcover (0.2 for Landsat 8 OLI and 0.35 for Sentinel-2 MSI; Appendix A). The team exported a layer of deciduousness from this approach. The results of the phenological approach were compared with both the 1954 stands and 2021 random forest output in ArcGIS Pro 3.0.2.

3.3.4 Change Comparison

The team converted the random forest and phenology raster outputs to polygons in ArcGIS Pro 3.0.2. After selecting polygons if they were within or intersected the historical digitized aspen stands, the team calculated the area of the selected modern aspen stands using the summary statistics tool, which was compared with the area of the historical aspen extent.

4. Results & Discussion

4.1 Analysis of Results

The team estimated an aspen extent of 9.45 km² from stands near the 113 belt transects in 1954 from the digitization of the historical imagery. Stands ranged in size from 457 m² to 2.83 km², with an average size of 0.08 km². In comparison, the Landsat 8 OLI random forest and phenological analysis resulted in an area range of 6.10 and 0.80 km² for aspen extent around the belt transects in 2021, respectively, and an area of 239.49 and 8.96 km² within the larger elk wintering range, respectively. The results from Sentinel-2 MSI analysis in the digitized area were 1.86 and 1.47 km² and 86.81 and 25.09 km² for the elk wintering range for random forest and phenology analysis, respectively. These results translated to a wide range of change calculations between 1954 and 2021 across the approaches (Table 1). Interestingly, the results from the two approaches for Landsat 8 OLI are both the largest and smallest estimations of aspen extent. These indicate the potential for over- and under-estimations likely related to the spatial resolution and pixels influenced by other landcover as well as the threshold set for the phenology approach. Sentinel-2's finer resolution resulted in less extreme predictions. Overall, all outcomes indicated a decline compared to the initial extent of 1954.

Table 1

Comparison of percent change of 113 aspen stands between 1954 digitization and 2021 methods

Method	Total Area (km²)	Change from 1954 (%)
1954 Digitization	9.45	n/a
2021 Landsat 8 OLI Random Forest	6.10	-35.45
2021 Sentinel-2 MSI Random Forest	1.86	-80.36
2021 Landsat 8 OLI Phenology	0.80	-91.57
2021 Sentinel-2 MSI Phenology	1.47	-84.40

The decline from 1954 to 2021 and improved delineation in 2021 from finer resolution imagery was evident when focusing on specific stands (Figures 2-4). In the example results, digitized extent can be seen for three stands. For those same three stands, the Landsat 8 OLI results show a coarse resolution, making it more difficult to pick out specific aspen boundaries. The overlap between the two approaches was evident in some places, which emphasized the limitations of both but also suggested increased confidence where there was overlap. With the Sentinel-2 imagery and results, delineations improved with the finer resolution. Again, in some locations, the two methods overlapped, resulting in greater confidence.

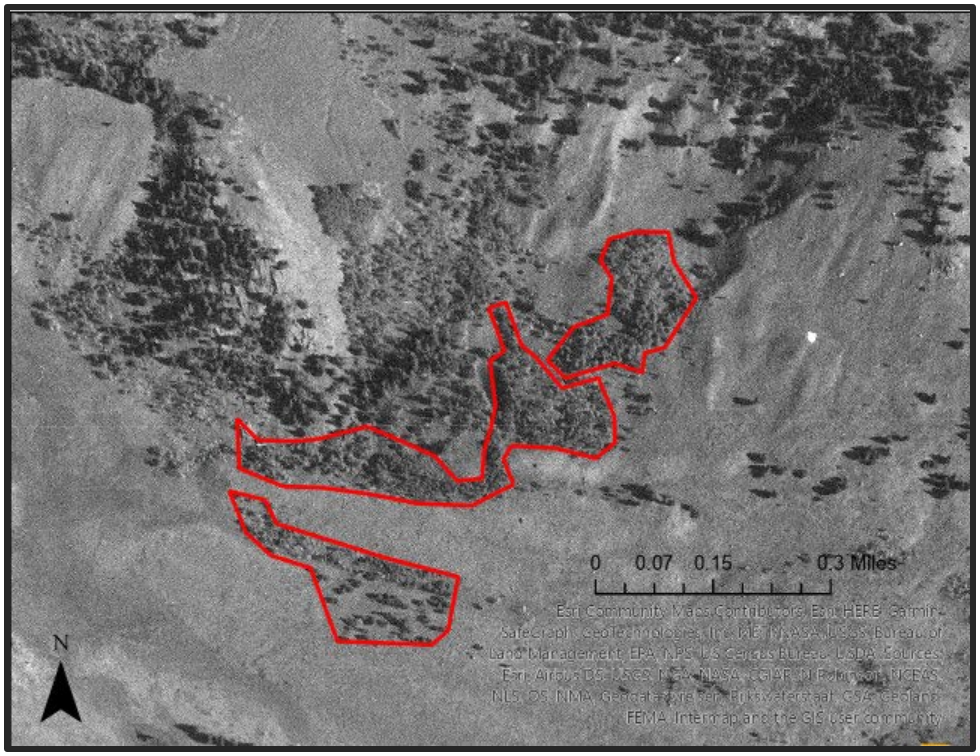

Figure 2. Digitized historical aspen extent (shown in red) for stands 14, 25, and 26.

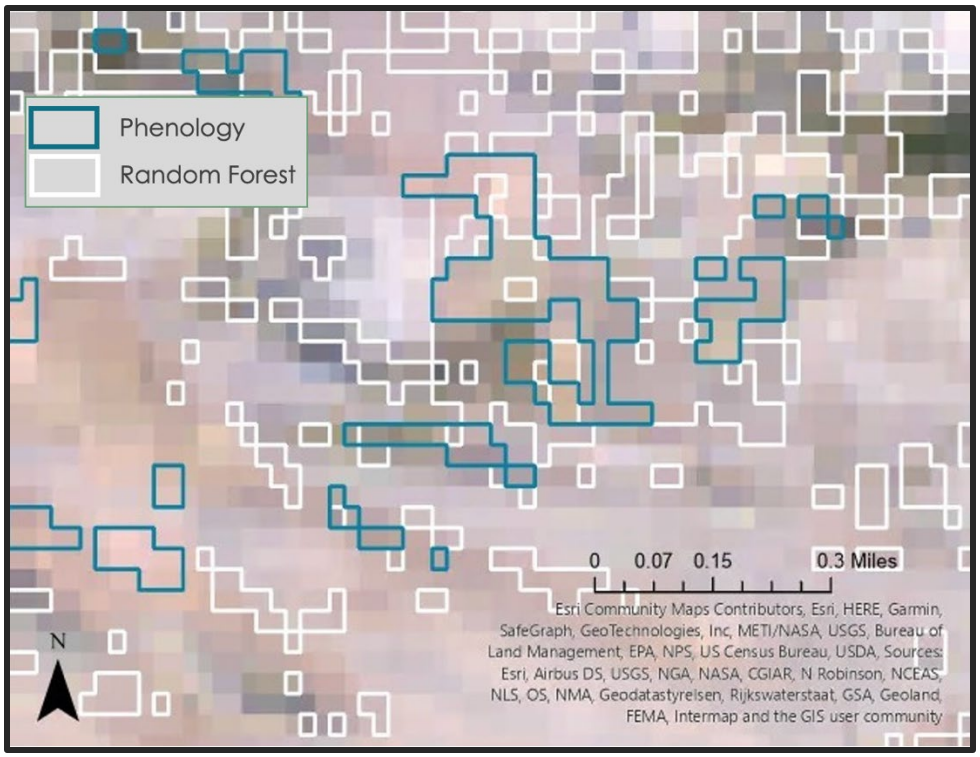

Figure 3. Random forest (white) and phenology (blue) aspen classification for belt transects 14, 25, and 26 using Landsat-8 OLI imagery. Areas where there is overlap indicate greater confidence in aspen presence.

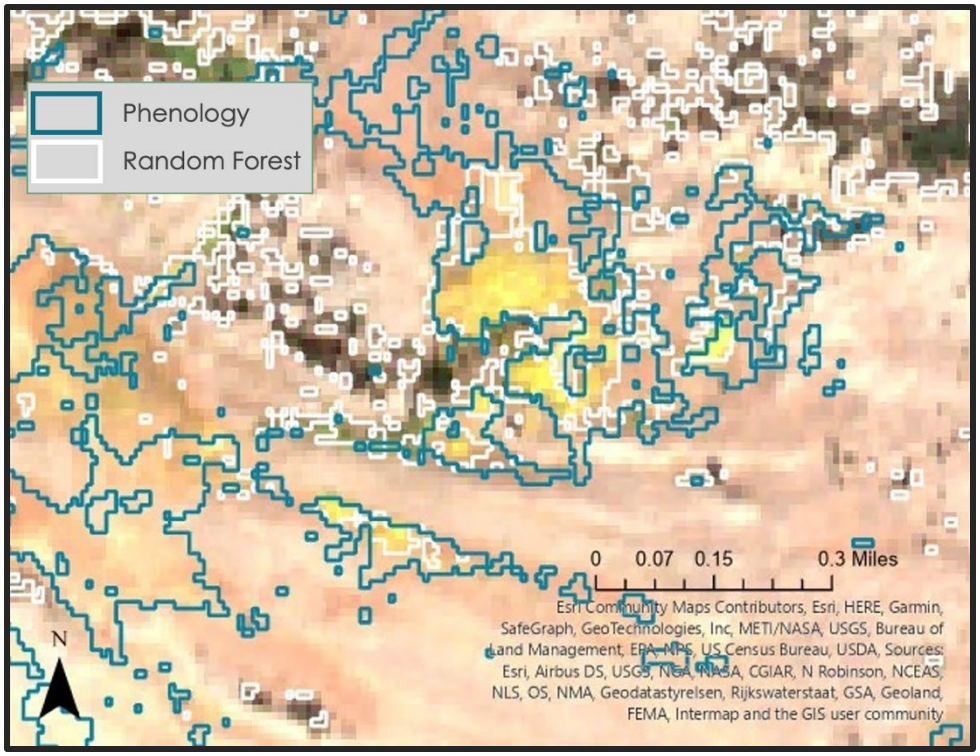

Figure 4. Random forest (white) and phenology (blue) aspen classification for belt transects 14, 25, and 26 using Sentinel-2 MSI imagery. Areas where there is overlap indicate greater confidence in aspen presence.

Confusion matrices for both Landsat 8 OLI and Sentinel-2 MSI random forest results (Appendix B) emphasized that the aspen class was most confused with the aggregated other vegetation class. In the validation set, some of the reference other vegetation was incorrectly identified as aspen, and some of the aspen was misidentified as other vegetation. As a result, these misidentifications caused both some over- and under-estimations in aspen area. The overall validation accuracy increased from 86.42% to 92.85% between Landsat 8 OLI and Sentinel-2 MSI results. Similarly, Cohen's kappa statistic also improved from 0.80 to 0.90 between the two sensors.

In comparison to the Summer 2022 DEVELOP team's results, the aspen extent for the elk wintering range is within estimations from 1986 to 2019. However, no clear pattern is evident as Landsat 8 OLI results differ greatly from each other. While Sentinel-2 results are not as extreme, all of the results are influenced by many of the choices made within the code (e.g., dates of imagery, NDVI threshold). The Summer 2022 DEVELOP team's random forest results were produced using summer imagery. For the fall 2022 term, the team decided to use fall imagery to capture leaf color change. The NDVI threshold in 2019 differed from that chosen for 2021. There are other slight differences that may influence the results, including the specific dates used. Many of these choices are necessary as year-to-year differences exist within the natural world. Because of this, comparing the results among sensors is difficult.

Due to georeferencing limitations of the 1954 imagery, it was difficult to compare 1954 to 2021, especially at the different scales that were being examined. Because the 1954 analysis focused on the 113 belt transects alone and the 2021 analysis focused on the entirety of the elk wintering range, there was a mismatch in comparing the area calculations, but the intersect with digitized stands was considered the best approach. Based on visual analysis as well, the team determined that aspen extent generally decreased from 1954 to 2021, contrary to what the partners had expected based on the trophic cascade.

While the general decrease in aspen stand extent could be associated with wolf-elk interactions, other factors could have had a stronger influence on the decline of aspen stands within the study area. For example, climate and more frequent and severe instances of wildfires and flooding in recent years could have decreased aspen stand extent in comparison to stands in 1954. Shifts in the population of other carnivores, such as grizzly bears (*Ursus arctos horribilis*) and cougars (*Puma concolor*), could also have effects on aspen extent and may have contributed to the decline seen in this analysis. Finally, more time could simply be needed to see aspen regeneration following wolf reintroduction in the 1990s.

4.2 Limitations

There is a large time gap between the 2019 NAIP imagery that the historical aerial imagery was referenced to and the 1954 imagery itself. While many of the features, such as ridges, would be unchanged, comparing other features, such as rivers, is problematic. Further, the team was not able to orthorectify 1954 imagery due to the lack of necessary metadata for the imagery.

Due to time constraints, the team was not able to analyze the same area in the 1990s during the beginning of wolf reintroduction in Yellowstone. Analysis of the selected aspen stands in the 1990s would have helped better understand the impacts that wolf reintroduction had and trend in aspen stands. As a result, the team was unable to fully determine the effects of wolves on the aspen population.

The random forest approach is advantageous for classifying land cover with accurate training points, while the phenological approach does not require them. However, random forest can target aspen more specifically, while phenology targets deciduous species in general. Used in combination, the two approaches can build confidence in areas that are likely aspen. The use of Sentinel-2 MSI imagery in addition to Landsat 8 OLI helps improve results since the finer resolution is closer to the size of aspen stands resulting in finer detail that is lost with Landsat 8 OLI. The coarse spatial resolution (30 m) of the Landsat 8 OLI imagery potentially results in over- or under-estimations of aspen extent since the pixels are influenced by other landcover types. The NDVI calculation for the phenological approach is based on available imagery, which may not be the ideal times of peak greenness and senescence due to revisit time and cloud cover issues. Additionally, using one threshold for NDVI change could misclassify deciduousness as stands could be found in microclimates that differ.

For Landsat 8 OLI, there was an error in the tasseled cap (wetness, brightness, and greenness) analysis. The team used B1 (ultra-blue) instead of B2 (blue) to begin the equation, shifting all other bands to the wrong coefficient. This error slightly impacted the random forest classification that is explained in this technical paper. When adjusted (the adjustment is not reflected in the numbers or figures included in this technical paper) the overall validation accuracy of the Landsat 8 OLI random forest classification decreased by less than 1%.

4.3 Future Work

The methodology used in this study could be refined by several means. First, in terms of aspen identification, specific bands and other indices could be utilized to see if the aspen signature within hyperspectral imagery is distinguishable from other similar landcover types. Alternative avenues to explore include focusing on other deciduous species in the region, like cottonwood and willow, to see if the trend applies to all deciduous species or aspen alone.

Several other research questions could be analyzed with the methodology used in this project. For example, since aspen are declining throughout North America due to several factors, another team could investigate if aspen in Yellowstone are affected not only by elk browsing, but by changes in temperature, moisture, and fire regimes as well as other biotic controls (e.g., pests and pathogens). Finally, the locations of die-off and regeneration could also be explored further to see if south- and west-facing slopes are more vulnerable as has been found elsewhere (Huang & Anderegg, 2012; Worrall et al., 2008).

5. Conclusions

Changes in aspen extent over the past several decades has had implications for ecosystem functioning and wilderness character in Yellowstone National Park. Utilizing historical aerial photographs and modern satellite imagery can enhance understanding of long-term ecological changes and inform resource management decision-making. The refined results from the random forest and phenological approaches allowed for detailed analysis of aspen extent in 2021. Combined with the extent determined from digitization of 1954 imagery, the team's analysis is particularly informative in the broader context of carnivore recovery in Yellowstone and its ecological impacts. Even though it is difficult to relate the results specifically to wolf reintroduction, correlations between aspen stand changes could be associated with time since rewilding decisions. Differences between the digitized 1954 and modeled 2021 aspen extent depict the landscape-scale changes that have taken place in Yellowstone. The results showed a general decrease in aspen stand extent since 1954. While other factors may have contributed to the decline, this analysis indicated aspen has not yet recovered from the decline seen after wolf extirpation. The team's analysis and end products open avenues for further research on the effects of trophic cascades and wildlife reintroductions.

6. Acknowledgments

The team would like to thank their partners: Dr. Daniel Stahler at Yellowstone National Park, Dr. Daniel MacNulty and Nicholas Bergeron at Utah State University, and Dr. Eric Larsen at the University of Wisconsin – Stevens Point for their engagement and guidance on this project. They would also like to thank their science advisors, Dr. Marguerite Madden and Joseph Spruce for their valuable insights in making this project a success. The team would also like to acknowledge their fellow, Sarah Payne, for her positive energy and suggestions throughout the term. Finally, this work would not have been possible without the work of the contributors during the Summer 2022 term.

This material contains modified Copernicus Sentinel data (2021), processed by ESA.

Any opinions, findings, and conclusions or recommendations expressed in this material are those of the author(s) and do not necessarily reflect the views of the National Aeronautics and Space Administration.

This material is based upon work supported by NASA through contract NNL16AA05C.

7. Glossary

3DEP – 3D Elevation Program
Digitization – The process of converting information, such as objects or images, into a digital format
Earth observations – Satellites and sensors that collect information about the Earth's physical, chemical, and biological systems over space and time
EVI – Enhanced Vegetation Index
GEE – Google Earth Engine
Georeferencing – Relating the internal coordinate system of a digital map or image to a geographic coordinate system by matching distinguishable points between the two
MODIS – Moderate Resolution Imaging Spectroradiometer
MSI – Multispectral Instrument
NAIP – National Agricultural Imagery Program
NDVI – Normalized Difference Vegetation Index
OLI – Operational Land Imager
Phenology – Cyclic or seasonal changes in natural systems
PlanetScope – Constellation of 130+ DOVE satellites, used to retrieve training data
Random forest model – Uses predictor variables and training points to create decision trees and determine classification
TCT – Tasseled Cap Transformation

Trophic Cascade – Top-down interspecific interactions that cause ecological effects at multiple levels within a food web

8. References

Baig, M.H.A., Zhang, L., Shuai, T., & Tong, Q. (2014). Derivation of a tasselled cap transformation based on Landsat 8 at-satellite reflectance. *Remote Sensing Letters*, *5*(5), 423-431. https://doi.org/10.1080/2150704X.2014.915434

Beschta, R. L., & Ripple, W. J. (2016). Riparian vegetation recovery in Yellowstone: the first two decades after wolf reintroduction. *Biological Conservation*, *198*, 93-103. https://doi.org/10.1016/j.biocon.2016.03.031

Brown, K., Hansen, A. J., Keane, R. E., & Graumlich, L. J. (2006). Complex interactions shaping aspen dynamics in the Greater Yellowstone Ecosystem. *Landscape Ecology*, *21*(6), 933-951. https://doi.org/10.1007/s10980-005-6190-3

Copernicus Sentinel-2 (processed by ESA), 2021, *MSI Level-2A BOA Reflectance Product*. Collection 1. European Space Agency. https://doi.org/10.5270/S2_-znk9xsj

Hamilton, R., Megown, K., DiBenedetto, J., Bartos, D., & Mileck, A. (2009). Assessing aspen using remote sensing. RSAC-0110-RPT2. Salt Lake City, UT: US Department of Agriculture, Forest Service, Remote Sensing Applications Center. 14 p.

Hayes, M., Miller, S., & Murphy, M. (2014). High-resolution landcover classification using Random Forest. *Remote Sensing Letters*, 5. https://doi.org/10.1080/2150704X.2014.882526

Huang, C.-Y., & Anderegg, W.R.L. (2012). Large drought-induced aboveground live biomass losses in southern Rocky Mountain aspen forests. *Global Change Biology*, *18*, 1016-1027. https://doi.org/10.1111/j.1365-2486.2011.02592.x

Huete, A., Justice, C., & Liu, H. (1994). Development of vegetation and soil indices for MODIS-EOS. *Remote Sensing of Environment*, *29*, 224–234. https://doi.org/10.1016/0034-4257(94)90018-3

Kauth, R. J. & Thomas, G. S. (1976). "The Tasselled Cap -- A Graphic Description of the Spectral-Temporal Development of Agricultural Crops as Seen by LANDSAT" (1976). *LARS Symposia*. Paper 159. https://docs.lib.purdue.edu/cgi/viewcontent.cgi?article=1160&context=lars_symp

Lamqadem A.A, Saber H, & Pradhan B. (2018). Quantitative Assessment of Desertification in an Arid Oasis Using Remote Sensing Data and Spectral Index Techniques. *Remote Sensing, 10*(12):1862. https://doi.org/10.3390/rs10121862

Larsen, E. J., & Ripple, W. J. (2005). Aspen stand conditions on elk winter ranges in northern Yellowstone, USA. *Natural Areas Journal*, *25*(4), 326. https://digitalcommons.usu.edu/aspen_bib/55

Painter, L. E., Beschta, R. L., Larsen, E. J., & Ripple, W. J. (2014). After long-term decline, are aspen recovering in northern Yellowstone? *Forest Ecology and Management*, *329*, 108-117. https://doi.org/10.1016/j.foreco.2014.05.055

Planet Team (2017). Planet Application Program Interface: In Space for Life on Earth. San Francisco, CA. https://api.planet.com

Ripple, W. J., & Beschta, R. L. (2012). Trophic cascades in Yellowstone: the first 15 years after wolf reintroduction. *Biological Conservation*, *145*(1), 205-213. https://doi.org/10.1016/j.biocon.2011.11.005

Ripple, W. J., & Larsen, E. J. (2000). Historic aspen recruitment, elk, and wolves in northern Yellowstone National Park, USA. *Biological Conservation*, *95*(3), 361-370. https://doi.org/10.1016/S0006-3207(00)00014-8

Ripple, W. J., & Larsen, E. J. (2001). The role of postfire coarse woody debris in aspen regeneration. *Western Journal of Applied Forestry*, *16*(2), 61-64. https://doi.org/10.1093/wjaf/16.2.61

Ripple, W.J., Larsen, E.J., Renkin, R.A., & Smith, D.W. (2001). Trophic cascades among wolves, elk and aspen on Yellowstone National Park's northern range. *Biological Conservation, 102*(3), 227-234. https://doi.org/10.1016/S0006-3207(01)00107-0

Rouse, J. W., Haas, R. H., Schell, J. A., & Deering, D. W. (1974). Monitoring vegetation systems in the Great Plains with ERTS. *NASA,* 1(A). https://ntrs.nasa.gov/citations/19740022614

Steen, K., Bailey., V., Boodhoo, G., & McLaughlin, B. (2022). *Yellowstone Ecological Forecasting: Assessing change in aspen extent in northern Yellowstone National Park* [Unpublished manuscript]. NASA DEVELOP National Program, Georgia – Athens.

USGS. (2020). Landsat 8 OLI Collection 2 Level-2 Science Products. [Data set]. USGS EROS Archive. https://doi.org/10.5066/f78s4mzj

USGS. (2017). USGS 1/3 arc-second n46w111 1 x 1 degree, 20171130. [Data set]. U.S. Geological Survey.

USGS. (2021). USGS 1/3 arc-second n45w111 1 x 1 degree, 20210615. [Data set]. U.S. Geological Survey.

Worrall, J.J., Egeland, L., Eager, T., Mask, R.A., Johnson, E.W., Kemp, P.A., & Shepperd, W.D. (2008). Rapid mortality of *Populus tremuloides* in southwestern Colorado, USA. *Forest Ecology and Management*, *255*, 686-696. https://doi.org/10.1016/j.foreco.2007.09.071

Appendix A

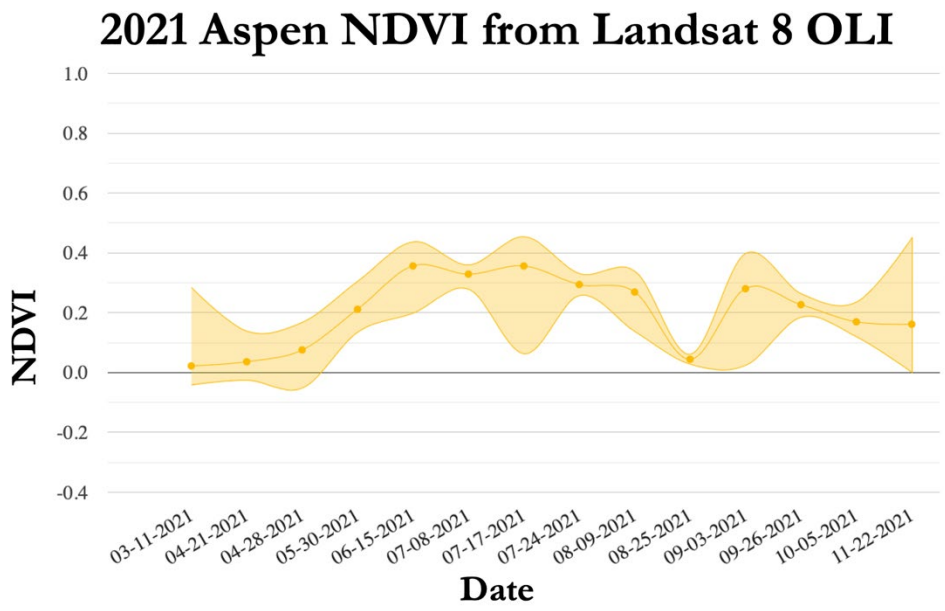

Figure A1. Mean NDVI for partner-provided aspen locations for 2021 from Landsat 8 OLI.

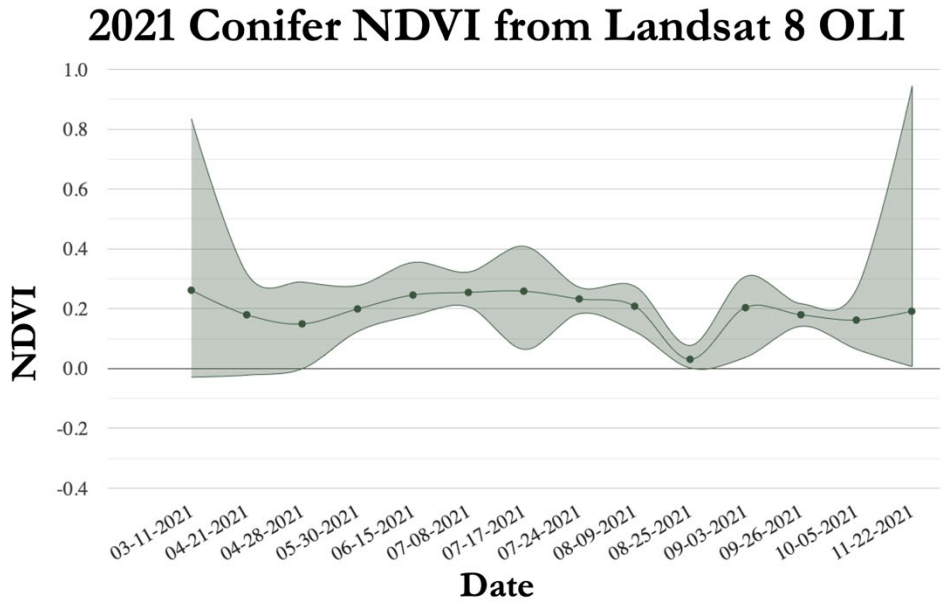

Figure A2. Mean NDVI for partner-provided conifer locations for 2021 from Landsat 8 OLI.

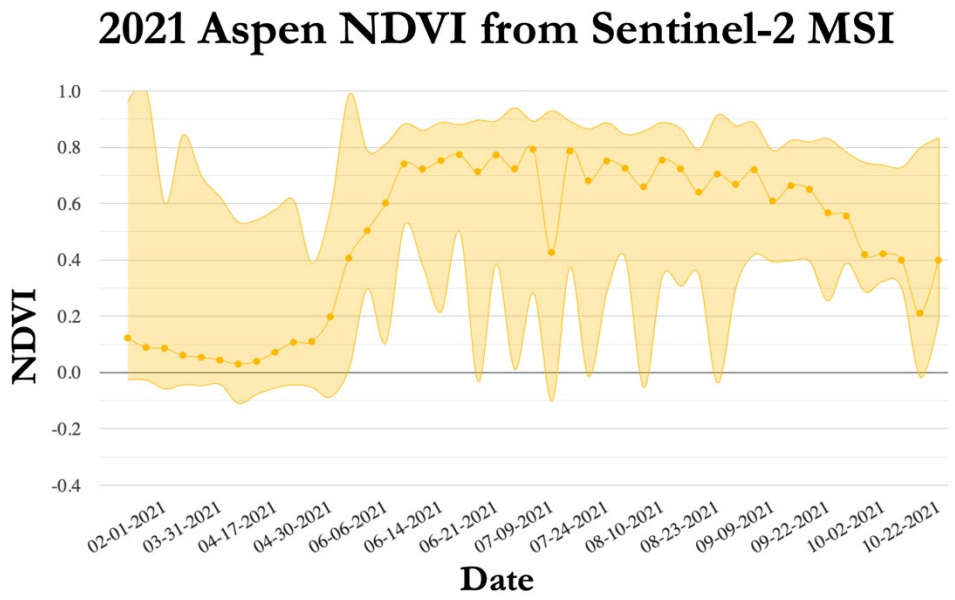

Figure A3. Mean NDVI for partner-provided aspen locations for 2021 from Sentinel-2 MSI.

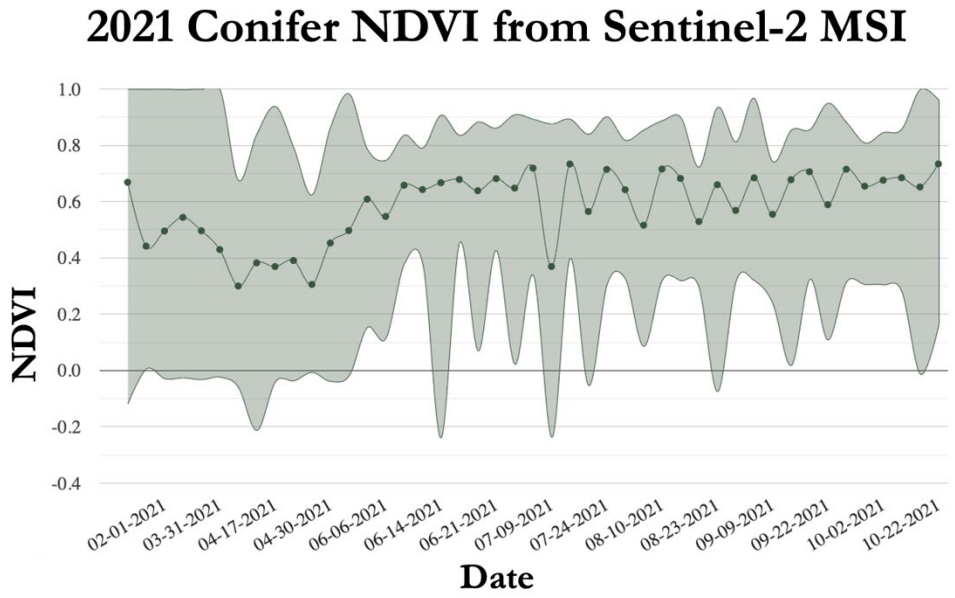

Figure A4. Mean NDVI for partner-provided conifer locations for 2021 from Sentinel-2 MSI.

Appendix B

Table B1

Confusion matrix for the 2021 Landsat 8 OLI random forest results

		Classified				
		Water	Bare Ground	Aspen	Conifer	Other Vegetation
Reference	Water	19	0	1	0	3
	Bare Ground	1	34	3	4	1
	Aspen	1	0	39	3	11
	Conifer	0	0	3	73	0
	Other Vegetation	2	3	16	0	166

Table B2

Confusion matrix for the 2021 Sentinel-2 MSI random forest results

		Classified				
		Water	Bare Ground	Aspen	Conifer	Other Vegetation
Reference	Water	26	0	0	0	2
	Bare Ground	1	30	0	6	0
	Aspen	0	0	48	0	13
	Conifer	0	0	0	82	1
	Other Vegetation	1	0	4	1	175